

1 **Magmatism of the Weddell Sea rift system in Antarctica: Implications for the**
2 **age and mechanism of rifting and early stage Gondwana breakup**

3

4

5 Teal R. Riley ^{a*}, Tom A.R.M. Jordan^a, Philip T. Leat^{a, b}, Mike L. Curtis^c, Ian L. Millar^d

6

7

8 ^a*British Antarctic Survey, High Cross, Madingley Road, Cambridge, CB3 0ET, UK*

9 ^b*Department of Geology, University of Leicester, University Road, Leicester, LE1 7RH, UK*

10 ^c*CASP, 181A Huntingdon Road, Cambridge, CB3 0DH, UK*

11 ^d*British Geological Survey, Keyworth, Nottingham, NG12 5GG, UK*

12

13

14

15

16

17

18

19 *Author for correspondence

20 e-mail: trr@bas.ac.uk

21 Tel. 44 (0) 1223 221423

22

23

24

25

26 **ABSTRACT**

27

28 Thick (~800 m) basaltic successions from the eastern Antarctic Peninsula have been dated in the
29 interval 180 – 177 Ma and preserve a transition from a continental margin arc to a back-arc
30 extensional setting. Amygdaloidal basalts from the Black Coast region of the eastern margin of the
31 Antarctic Peninsula represent a rare onshore example of magmatism associated with back-arc
32 extension that defines the early phase of Weddell Sea rifting and magmatism, and Gondwana
33 breakup. The early phase of extension in the Weddell Sea rift system has previously been
34 interpreted to be related to back-arc basin development with associated magnetic anomalies
35 attributed to mafic-intermediate magmatism, but with no clearly defined evidence of back-arc
36 magmatism. The analysis provided here identifies the first geochemical evidence of a transition from
37 arc-like basalts to the development of depleted back-arc basin basalts in the interval 180 – 177 Ma.
38 The exposed Black Coast basaltic successions are interpreted to form a minor component of
39 magmatism that is also defined by onshore sub-ice magnetic anomalies, as well as the extensive
40 magnetic anomalies of the southern Weddell Sea. Back-arc magmatism is also preserved on the
41 Falkland Plateau where intrusions postdating 180 Ma are associated with early phase rifting in the
42 Weddell Sea rift system. Back-arc extension was probably short-lived and had ceased by the time the
43 northern Weddell Sea magmatism was emplaced (<175 Ma) and certainly by 171 Ma, when an
44 episode of silicic magmatism was widespread along the eastern Antarctic Peninsula. Previous
45 attempts to correlate mafic magmatism from the eastern Antarctic Peninsula to the Ferrar large
46 igneous province, or, as part of a bimodal association with the Chon Aike silicic province are both
47 dismissed based on age and geochemical criteria.

48

49 **Keywords:** Gondwana; back-arc extension; basalts; Ferrar; large igneous province

50 **1. Introduction**

51

52 The evolution of the Weddell Sea rift system (WSRS) is closely linked with the emplacement of
53 the Karoo-Ferrar large igneous province (LIP), the early breakup of Gondwana, and the translation
54 and rotation of micro-continental blocks that formed West Antarctica (Schopf, 1969). The WSRS
55 developed on the continental lithosphere of Antarctica (Leat et al., 2018) and interpretation of
56 aeromagnetic geophysical data (Ferris et al., 2000; Jordan et al., 2013, 2017) and seismic data (Jokat
57 and Herter, 2016) indicates that large parts of the present day Weddell Sea are underlain by mafic
58 intrusions/lavas. The magmatism of the WSRS has been attributed to an offshore extension of the
59 Early Jurassic Ferrar LIP (Storey et al., 1996), magmatism associated with rifting during the early
60 stages of Gondwana breakup (e.g. Martin, 2007) or a failed Jurassic ocean basin (Jokat and Herter,
61 2016). Two separate episodes of Weddell Sea extension and magmatism have been identified by
62 several authors (e.g. König and Jokat, 2006; Jordan et al., 2017); an early stage east-west rifting
63 episode potentially linked to back-arc extension and a later stage north-south rifting episode
64 associated with the separation of Antarctica and Africa.

65 This paper investigates the petrogenesis and tectonic setting of thick (500 – 800 m) successions of
66 Early Jurassic basaltic volcanic rocks from the eastern Antarctic Peninsula and how they relate to
67 early stage extension as part of the WSRS. We shall evaluate if the basaltic magmatism is related to
68 back-arc rifting associated with the Antarctic Peninsula continental margin and how this relates to
69 Weddell Sea rifting, or whether the mafic magmatism is more closely related to the Ferrar LIP.

70

71 **2. Weddell Sea Rift System**

72

73 *2.1 Overview*

74

75 The Weddell Sea and embayment is bounded by the Antarctic Peninsula, East Antarctica and the
76 smaller crustal blocks of Haag Nunataks and the Ellsworth-Whitmore Mountains to the south (Fig. 1).
77 The precise position of these microcontinental crustal blocks in the developing Weddell Sea prior to
78 and during fragmentation of the Gondwana supercontinent are still not resolved (e.g. Dalziel, 2013;
79 Jordan et al., 2017; Jokat and Herter, 2016), particularly their translation and rotation. Based on
80 geological and paleomagnetic data the crustal blocks are suggested to be translated from a pre-
81 breakup position towards the Natal Embayment between East Antarctica and South Africa (Dalziel
82 2013, Randall and MacNiocaill 2004). Alternatively, models suggesting far more limited rotation and
83 translation are interpreted from geophysical investigations of the WSRS area, which do not exhibit
84 any tectonic evidence for a far-traveled block (Studinger and Miller, 1999; Jokat and Herter 2016;
85 Jordan et al., 2017). The motion of the Haag Nunataks and Ellsworth-Whitmore Mountains crustal
86 blocks are key to understanding the evolution of West Antarctica and the WSRS as their movement
87 involved interaction with the WSRS, but the mechanism of this relationship is poorly understood.
88 Jordan et al. (2013) interpreted the WSRS to be 400 – 600 km in width along most of its 900 km
89 length, but widening towards the north where there is a transition from thinned continental crust to
90 oceanic crust of the Weddell Sea embayment (King, 2000). Seismic refraction data along the front of
91 the Filchner-Ronnie Ice Shelf identifies a zone of ~20 km thick crust overlain by 12 – 15 km of
92 sediments (Leitchenkov and Kudryavtzev, 1997; Jokat and Herter, 2016), interpreted to reflect
93 anomalously thick oceanic crust or highly attenuated, underplated and intruded transitional
94 continental crust (Jokat and Herter, 2016). These seismic estimates of crustal thickness are
95 consistent with regional estimates from gravity data of <30 km from GRACE satellite data (Block et
96 al., 2009), and 27 – 29 km from marine and terrestrial gravity data (Studinger and Miller 1999).

97 Jordan et al. (2017) divided the WSRS into two distinct provinces identified by their differently
98 trending magnetic anomalies (Fig. 3a). The Northern Weddell magnetic province (NWMP) is
99 characterized by magnetic anomalies with a prominent NE-SW trend (Fig. 3b). A Southern Weddell
100 magnetic province (SWMP) which is situated between the Haag Nunataks crustal block and the

101 Explora Anomaly (Fig. 3b) has magnetic anomalies with a dominant N-S trend. Jordan et al. (2017)
102 interpreted the SWMP to predate the NWMP on the basis of cross-cutting trends. They suggested
103 that the SWMP related to Early Jurassic east-west extension in the WSRS that may have been linked
104 to back-arc extension along the Antarctic Peninsula margin. Nevertheless, they were unable to
105 identify any clear evidence for back-arc related magmatism. The NE-SW trending NWMP is
106 characterized by a fault splay magnetic fabric. This has been interpreted to be related to the
107 separation of East Antarctica and Africa (Jordan et al., 2017), although a component of
108 approximately N-S rifting between the Antarctic Peninsula and East Antarctica is suggested from
109 seismic data (Jokat and Herter 2016), and is required if the Antarctic Peninsula was in its current
110 location. The nature of the crust in the NWMP is not resolved by potential field data, but the highly
111 extended transitional continental, or anomalously thick oceanic crust, observed in seismic refraction
112 data (Jokat and Herter 2016) is consistent with the NWMP having undergone significant extension
113 and rifting. The higher amplitude of the observed magnetic anomalies, relative to the SWMP region,
114 may reflect the more magmatic and closer to oceanic character of this region.

115

116 *2.2 Age of rifting*

117

118 The age of rifting of the WSRS has not been dated directly, but is considered to be Early – Middle
119 Jurassic in age, overlapping with the early stages of Gondwana breakup (Storey et al., 1988; König
120 and Jokat, 2006; Martin, 2007; Dalziel, 2013; Jordan et al., 2017; Leat et al., 2018). Jordan et al.
121 (2017) interpreted the east-west rifting of the SWMP to be related to back-arc extension along the
122 Antarctic Peninsula margin. They suggested that this extension was accommodated along the
123 geophysically identified Pagano shear zone on the Ellsworth-Whitmore Mountains block to the south
124 (Fig. 3b). The Pagano shear zone is interpreted to be a left lateral transtensional structure (Jordan et
125 al., 2013) with ~500 km of displacement (Jordan et al., 2017). Movement on the shear zone has been
126 dated at ~175 Ma, based on the age of Early Jurassic syn-deformational plutons that were emplaced

127 in the interval 178 – 174 Ma (Lee et al., 2012; Jordan et al., 2013; Craddock et al., 2017; Leat et al.,
128 2018). The Pagano Nunatak granite (Fig. 1; 174.62 ± 0.16 Ma; Craddock et al., 2017) was emplaced in
129 a releasing bend of the Pagano shear zone near the margin of the Ellsworth-Whitmore Mountains
130 block, implying that the shear zone was active at this time. Other associated granites at Pirrit Hills
131 (178.0 ± 3.5 Ma; Leat et al., 2018), Nash Hills (177.44 ± 0.04 Ma; Craddock et al., 2017) and Linck
132 Nunatak (174.382 ± 0.26 Ma; Craddock et al., 2017) do not show any direct evidence of
133 emplacement into an active shear zone and are adjudged to have been emplaced within the more
134 coherent Ellsworth-Whitmore Mountains crustal block (Jordan et al., 2013; Leat et al., 2018). If
135 motion on the Pagano shear zone was related to east-west extension as part of the SWMP (Jordan et
136 al., 2017) then the deformed granitoid emplacement age from Pagano Nunatak (174.6 ± 0.2 Ma)
137 should provide a reliable chronometer for the initial phase of Weddell Sea rifting and the early
138 stages of Gondwana breakup.

139 Storey et al. (1988) and Leat et al. (2018) considered that lithospheric extension in the WSRS led
140 to extensive mafic magmatism, which allowed the development of a thickened lower crustal
141 underplate, providing heat for crustal anataxis and the emplacement of the Pagano shear zone
142 granites.

143 Dating the age of rifting that led to the development of the NWMP is more difficult as there are
144 no clear onshore examples of magmatic or tectonic activity associated with the broadly northwest-
145 southeast extension. Cross-cutting relationships of magnetic fabrics indicate the NWMP postdates
146 the ~ 175 Ma extension of the SWMP (Jordan et al., 2017), whilst rifting of the NWMP is likely to have
147 predated the development of true oceanic crust in the Weddell Sea embayment.

148 Identifying the age of oceanic crust in the Weddell Sea is complicated because of slow spreading
149 rates, which makes identifying magnetic anomaly ages difficult. König and Jokat (2006) interpreted
150 the first true ocean floor in the southern Weddell Sea to have been created at ~ 147 Ma (M19/M20
151 chron) following approximately 20 Myr of stretching and rifting in the WSRS. Although Jokat and
152 Herter (2016) suggested that the maximum age of oceanic crust could be ~ 160 Ma. If the ~ 147 Ma

153 age is correct for the earliest oceanic spreading, the rifting that led to the development of the
154 NWMP is interpreted to have taken place in the interval 175 – 147 Ma. Mueller and Jokat (2019)
155 have investigated magnetic spreading anomalies constraining oceanization in the Africa-Antarctica
156 corridor and have identified anomalies as old as 164 Ma, but these ages may not continue in to the
157 Weddell Sea sector.

158

159 *2.3 Summary of WSRS events*

160

161 Extension in the Weddell Sea sector of Antarctica was a critical episode in the early stages of
162 Gondwana breakup and records evidence of rifting between East and West Antarctica and
163 separation of Antarctica from Africa and South America. It also played a pivotal role in the
164 distribution of smaller crustal blocks during breakup and West Antarctica assembly.

165 The geology of the present day Weddell Sea has been influenced by five key events during the
166 early stages of Gondwana breakup:

- 167 i) *The emplacement of the Karoo-Ferrar LIP at 183 ± 1 Ma (U-Pb ages: Svensen et al., 2012;*
168 *Burgess et al., 2015).* This major magmatic event is thought to have been related to
169 early-formed rift structures associated with the first stages of Gondwana breakup, both
170 between Africa and Antarctica, and in the Weddell Sea embayment (Elliot and Fleming,
171 2000). The magmatism may be related to the Filchner rift and Explora magnetic
172 anomalies (Fig. 3), which are interpreted to be the oldest structures identified in the
173 southern Weddell Sea (Ferris et al., 2000).
- 174 ii) *Early Jurassic (~180 – 175 Ma) rifting leading to the SWMP.* This episode of east-west
175 extension and magmatism was one of the earliest phases of Gondwana breakup in the
176 Weddell Sea sector and has been linked to back-arc basin extension of the Antarctic
177 Peninsula associated with slab roll-back and trench retreat. Movement associated with

178 east-west extension of the SWMP was accommodated along the Pagano shear zone
179 (Jordan et al., 2017).

180 iii) *Middle – Late Jurassic rifting of the NWMP is related to the early stages of separation of*
181 *East Antarctica and South America.* NE-SW trending magnetic anomalies, semi-parallel
182 to the Explora Anomaly (Fig. 3), record magmatism associated with crustal thinning. This
183 episode of extension postdates the SWMP.

184 iv) *Development of oceanic crust in the northern Weddell Sea embayment.* Developed as a
185 result of seafloor spreading that initiated at ~147 Ma and accelerated through the
186 Cretaceous as rifting between Antarctica and South America continued and led to the
187 development of the Rocas Verdes marginal basin (Mukasa and Dalziel, 1996).

188 v) *Subduction of Weddell Sea oceanic crust at the active margin with the emerging Scotia*
189 *Plate.* The subduction zone would have developed to the south and east of the present
190 day South Scotia Ridge and led to the subduction of the northern flank of the Weddell
191 Sea oceanic crust (Barker, 2001).

192

193 *2.4 Role of crustal blocks in the developing Weddell Sea*

194

195 The WSRS is closely associated with the translation and potential rotation of the
196 microcontinental blocks of Haag Nunataks and Ellsworth-Whitmore Mountains (e.g. Jordan et al.,
197 2017; Dalziel, 2013). The crustal blocks translated and rotated from their pre-breakup position in the
198 Natal Embayment (Fig. 2) between East Antarctica and South Africa (Adie, 1952; Schopf, 1969;
199 Dalziel and Elliot, 1982; Grunow et al., 1987; Curtis and Storey, 1996). Jordan et al. (2017)
200 interpreted the Haag Nunataks and Ellsworth-Whitmore microcontinents to be a composite crustal
201 block whose movement was associated with extension in the WSRS during the breakup of
202 Gondwana.

203

204 **3. Influence of the Ferrar LIP on Weddell Sea rift magmatism**

205

206 *3.1 Background*

207

208 The Ferrar LIP extends along the length of the Transantarctic Mountains from the Theron
209 Mountains to northern Victoria Land (Fig. 1; Elliot et al., 1999). Magmatism of the Ferrar LIP has also
210 been recognized from southeast Australia (Hergt et al., 2001), New Zealand (Mortimer, 1995),
211 southern Africa (Riley et al., 2006) and potentially the Falkland Islands (Hole et al., 2016). The total
212 length of the Ferrar LIP is over 4000 km and outcrops mostly as extensive sill complexes, often with
213 thicknesses of up to 200 m (Elliot and Fleming, 2000). Chemical homogeneity over large distances of
214 the Ferrar LIP has led Fleming et al. (1997) and Leat (2008) to advocate the long distance transport of
215 Ferrar magmas.

216 The Dufek Massif and Forrestal Range layered mafic intrusion (Fig. 1) has an estimated volume of
217 $\sim 6600 \text{ km}^3$ (Ferris et al., 1998) and has been interpreted to form part of the Ferrar LIP and may
218 represent one of the point sources for the long distance transport of magmas via a network of sills or
219 dykes (Leat, 2008).

220 The Ferrar LIP lavas and sills are predominantly low-Ti tholeiites and have been dated by several
221 workers (Fleming et al., 1997), but often with concerns over the accuracy of the $^{40}\text{Ar}/^{39}\text{Ar}$
222 geochronology (Riley and Knight, 2001). Recent, high precision dating by Burgess et al. (2015) have
223 resolved the geochronology from large areas of the Ferrar LIP into the narrow time interval, 183.2 –
224 $182.8 \pm 0.2 \text{ Ma}$. The Dufek layered mafic intrusion has also been dated by Burgess et al. (2015) and
225 yielded a $^{206}\text{Pb}/^{238}\text{U}$ age of $182.7 \pm 0.1 \text{ Ma}$, consistent with the U-Pb age of $182.7 \pm 0.4 \text{ Ma}$
226 determined by Minor and Mukasa (1997).

227

228 *3.2 Gondwana breakup magmatism and the Weddell Sea rift*

229

230 The coincidence in age between magmatism of the Karoo (182 ± 2 Ma; Svensen et al., 2012) and
231 the Ferrar (183 ± 1 Ma; Burgess et al., 2015) magmatic provinces, and the early stages of Gondwana
232 breakup and Weddell Sea rifting have led several authors (e.g. Storey et al., 1996) to propose an
233 extension of LIP magmatism into the Weddell Sea region. Several authors (e.g. Ferris et al., 2000;
234 Elliot and Fleming, 2000; König and Jokat, 2006; Jokat and Herter, 2016) interpreted the WSRS to be a
235 failed arm of the Jurassic triple junction that formed above a mantle plume which led to LIP
236 emplacement (Elliot and Fleming, 2000; Storey et al., 2013). The Explora Anomaly of the coastal
237 margin of East Antarctica (Fig. 3b) is also interpreted to be related to breakup magmatism at ~ 183
238 Ma (Jourdan et al., 2005), whilst Jordan et al. (2017) suggested the parallel trending NWMP could
239 also be related to Karoo-Ferrar magmatism.

240 Karoo-Ferrar magmatism recorded from KwaZulu Natal ($182 - 176$ Ma; Riley et al., 2006), the
241 Falkland Islands ($182 - 179$ Ma; Hole et al., 2016) and the orientation of the magnetic anomalies of
242 the NWMP may indicate an expression of Karoo-Ferrar magmatism that extends across this region of
243 pre-breakup Gondwana (Fig. 2), with an extension onto the eastern Antarctic Peninsula (Fig. 4).
244 However, establishing any clear correlation between Karoo-Ferrar LIP magmatism and Weddell Sea
245 magmatism is complicated by the absence of any precise age control on Weddell Sea rift-related
246 magnetic anomalies of the NWMP, although the broader age range of magmatism ($182 - 176$ Ma)
247 from KwaZulu Natal (Riley et al., 2006) and the Falkland Islands (Hole et al., 2016) is perhaps more
248 conducive of a link to the NWMP. However by understanding the petrogenesis and tectonic setting
249 of the basaltic magmatism on the eastern Antarctic Peninsula it is possible to resolve how
250 widespread Karoo-Ferrar magmatism was in the WSRS.

251

252 **4. Antarctic Peninsula magmatism**

253

254 *4.1 Geology of the Antarctic Peninsula*

255

256 The Antarctic Peninsula has been interpreted as an accretionary continental arc of the
257 Gondwanan margin, which developed on Paleozoic basement during Mesozoic subduction (Suarez,
258 1976). Vaughan and Storey (2000) reinterpreted the geology of the Antarctic Peninsula as an
259 amalgamation of para-autochthonous and allochthonous terranes which accreted onto the Gondwana
260 margin. More recently, Burton-Johnson and Riley (2015) have suggested a tectonic model involving
261 in situ continental arc development and have rejected an accreted terrane hypothesis.

262 The geology of the eastern margin of the Antarctic Peninsula is dominated by Early – Middle
263 Jurassic silicic volcanic rocks (Pankhurst et al., 2000; Riley et al., 2001), which are closely associated
264 with granitoid plutonic rocks (Riley and Leat, 1999), thick (~1 km) sequences of Jurassic terrestrial
265 sedimentary rocks deposited in a back-arc basin (Hunter et al., 2005) and significant basaltic units
266 (Wever and Storey, 1992; Riley et al., 2016). These Jurassic sequences are thought to overlie
267 metamorphic and plutonic rocks of Paleozoic age based on broadly distributed isolated outcrops
268 (e.g. Riley et al., 2012).

269

270 *4.2 Basaltic lava successions*

271

272 Basaltic lavas and mafic greenstones crop out at multiple localities along the eastern margin of
273 the Antarctic Peninsula and have been described by Wever and Storey (1992) and Riley et al. (2003,
274 2016) from Jason Peninsula and the Black Coast-Lassiter Coast region of eastern Palmer Land (Fig. 1).

275 The greatest observed thicknesses of Jurassic basaltic lavas on the eastern Antarctic Peninsula
276 (Fig. 1) occur at the Eland Mountains (>800 m thickness) and Kamenev Nunataks (>500 m) where
277 weakly porphyritic, deformed amygdaloidal metabasalts crop out (Fig. 5). The unit at Eland
278 Mountains has been described by Riley et al. (2016) and was interpreted as a succession of basaltic
279 lava flow units. The lavas are metamorphosed to greenschist facies and contain leucocratic
280 amygdales, which are ovoid - irregular in form. The basaltic groundmass is characterized by
281 abundant plagioclase and actinolite, with minor epidote and titanite. The lavas are punctuated by

282 several fine grained, cream-grey coloured felsic units, which are typically 1 – 2 m in thickness and
283 were emplaced contemporaneously with the basaltic lavas. These felsic units have been dated by
284 Riley et al. (2016) at 180.2 ± 0.7 and 177.6 ± 1.0 Ma and provide an age for the entire basaltic
285 succession at 178 ± 2 Ma. This age is broadly coincident with the age of the basaltic lavas from Jason
286 Peninsula (main phase 176 – 174 Ma; Riley et al., 2003) and the age of basaltic lavas from the
287 Sweeney Formation further south, which were interpreted to be younger than 183 Ma based on
288 detrital zircon ages from associated metasedimentary rocks (Hunter et al., 2006). Therefore, a
289 significant pulse of basaltic magmatism within the age range, 183 – 176 Ma, with a probable age of
290 ~ 178 Ma is widespread along the eastern margin of the Antarctic Peninsula.

291 Previous workers (e.g. Riley et al., 2003) have attempted to correlate the Early Jurassic basaltic
292 magmatism with the extensive silicic volcanism of the region (Riley et al., 2001, 2010). However,
293 silicic volcanism occurred in two distinct pulses on the Antarctic Peninsula at ~ 184 – 183 Ma and 171
294 – 168 Ma (Pankhurst et al., 2000; Hunter et al., 2006; Riley et al., 2010), so it is difficult to include the
295 episode of basaltic magmatism at ~ 178 Ma into either of these events and a distinct tectonic
296 environment is now favoured.

297

298 *4.3 Evidence of mafic magmatism from geophysical data*

299

300 McGibbon and Wever (1991) identified a series of north-south trending magnetic anomalies
301 across eastern Palmer Land, from the Black Coast towards the Filchner-Ronne Ice Shelf (Fig. 1). Using
302 the magnetic susceptibilities recorded by McGibbon and Garrett (1987), McGibbon and Wever
303 (1991) were able to interpret that the north-south trending magnetic anomalies (Fig. 3b) could only
304 be the result of either gabbroic rocks or amygdaloidal basalts of the known lithologies that outcrop
305 on the adjacent eastern Antarctic Peninsula. The basaltic lava/gabbroic bodies that occur in the
306 coast parallel north-south trending zone are likely to have had a strong tectonic control on their
307 emplacement, potentially as a result of east-west extension. They are likely to represent a significant

308 offshore and sub-ice extension of the basaltic rocks identified from Eland Mountains-Kamenev
309 Nunatak.

310

311 **5. Geochemistry**

312

313 *5.1 Previous work*

314

315 Riley et al. (2003, 2016) and Wever and Storey (1992) investigated the geochemistry of the
316 basaltic units from Eland Mountains, Kamenev Nunatak and Jason Peninsula (Fig. 1). These mafic
317 rocks from the eastern Antarctic Peninsula exhibit only a moderate degree of variation; the Eland
318 Mountains succession are overwhelmingly transitional basalts akin to the Group III basalts from the
319 Black Coast (Wever and Storey, 1992). The lavas from Kamenev Nunatak are calc-alkaline and more
320 intermediate in composition, akin to the basaltic andesites from Jason Peninsula (Riley et al., 2003).
321 The Th/Yb vs. Nb/Yb plot (Fig. 6) which uses trace elements that are likely to have been immobile
322 during alteration and metamorphism is a useful diagram to illustrate the influence of subduction-
323 modified components relative to MORB-OIB compositions. A subset of Eland Mountains and
324 Kamenev Nunatak basaltic lavas are close in composition to the basaltic andesites of the Ferrar LIP
325 and have relatively high Th/Yb with respect to MORB-OIB, typical of compositions from continental
326 margin arcs. This attribute is even more marked in the intermediate rocks of Jason Peninsula which
327 have the highest Th/Yb ratios (~5). The field defined by the Black Coast Cretaceous dykes (Leat et al.,
328 2002) is used to represent mafic magmas derived from subduction-modified lithospheric mantle in
329 the Antarctic Peninsula and overlaps with the most enriched rocks of the Eland Mountains-Kamenev
330 Nunatak succession.

331

332 *5.2 Analytical techniques*

333

334 Five basaltic samples from Eland Mountains, Kamenev Nunatak and the nearby Leininger Peak
335 (Fig. 1) have been analysed for their Sr-Nd isotope values (Table 1). Sr and Nd isotope compositions
336 were measured at the British Geological Survey (Keyworth, UK) where samples were dissolved using
337 standard HF/HNO₃ methods. Sr and bulk REE were separated using Dowex AG50 cation exchange
338 columns, and Nd was subsequently extracted using LN-Spec columns. Sr fractions were loaded onto
339 outgassed single Re filaments using a TaO activator solution, and analysed in a Thermo-Electron
340 Triton mass spectrometer in multi-dynamic mode. Data are normalised to $^{86}\text{Sr}/^{88}\text{Sr} = 0.1194$. Results
341 are quoted relative to a value of 0.710250 for the NBS987 standard. Nd fractions were loaded onto
342 one side of an outgassed double Re filament assembly, and analysed in a Thermo Scientific Triton
343 mass spectrometer in multi-dynamic mode. Data are normalised to $^{146}\text{Nd}/^{144}\text{Nd} = 0.7219$. Results
344 are quoted relative to a value of 0.512115 for the JNd-i standard.

345

346 *5.3 Interpretation*

347

348 Analysis of the geochemistry of basaltic rocks from the eastern Antarctic Peninsula illustrates that
349 more than half of the analysed samples (Wever and Storey, 1992; Riley et al., 2016; this study) from
350 the Eland Mountains-Kamenev Nunatak succession plot at much more depleted compositions close
351 to the MORB array, and overlap in Nb/Yb with N-MORB. The compositions of these samples is
352 consistent with a sub-lithospheric MORB-like source mantle, perhaps melting in an extensional
353 setting. The modest increase in Th/Nb relative to N-MORB suggests a back-arc setting (Pearce and
354 Stern, 2006). The amygdaloidal basaltic rocks from the Hjort Formation (Wever and Storey, 1992)
355 and the Sweeney Formation (Hunter et al., 2006) also overlap with the more depleted basaltic rocks
356 from Eland Mountains-Kamenev Nunatak, also supporting a possible back-arc extensional setting.

357 The plot of Ba/Nb vs. Th/Nb (Fig. 7) is a useful discriminant to understand the relative
358 contribution of different source components in arc and back-arc extensional settings. Ba/Nb is a
359 proxy for the contribution from the arc, whilst Th/Nb provides a proxy for a deeper contribution. A

360 diagonal vector reflects both Th and Ba enrichment, whilst the vertical vector reflects only Ba
361 shallow enrichment (Pearce and Stern, 2006). Caution has to be exercised using Ba as a discriminant,
362 given its mobility, so the least altered rocks have been selected for analysis. A subset of the lavas
363 from the Eland Mountains succession closely follow the deep component vector, typical of a back-
364 arc extensional setting and are the samples that plot at depleted compositions in Fig. 6. The
365 Cretaceous dykes of the Antarctic Peninsula (Leat et al., 2002) follow the shallow enrichment vertical
366 vector and represent the geochemical characteristics of the Antarctic Peninsula magmatic arc. The
367 lavas from Jason Peninsula are distinct to both the Antarctic Peninsula arc dykes and the Eland
368 Mountains-Kamenev Nunatak and may reflect emplacement in a developing extensional setting that
369 isn't apparent in Fig. 6. The basaltic rocks from the Hjort Formation and Sweeney Formation are also
370 close to the deep component vectors indicating a potential back-arc extensional setting as suggested
371 in Fig. 6. Rare earth element (REE) values also demonstrate the relatively depleted characteristics of
372 a subset of basaltic rocks from Eland Mountains and the Sweeney Formation, in comparison to the
373 Black Coast Cretaceous dykes and the basaltic andesites from Jason Peninsula (Fig. 8). The Eland
374 Mountains and Sweeney Formation basalts have relatively flat REE profiles, indicating derivation
375 from a more depleted source, in comparison to the strongly enriched REE profiles from Jason
376 Peninsula and the Cretaceous dykes, which are typical of derivation from a subduction-modified
377 source.

378 The newly acquired dataset is plotted alongside Sr-Nd data (Fig. 9) from other Black Coast basaltic
379 rocks (Wever and Storey, 1992). Also plotted are the field of mafic rocks from the Ferrar LIP (Fleming
380 et al., 1995; Molzahn et al., 1996) and potentially related magmatism from the Falkland Islands (Hole
381 et al., 2016) and KwaZulu Natal (Riley et al., 2006). The limited isotopic dataset from the Eland
382 Mountains-Kamenev Nunatak region exhibit a broad range in both $^{87}\text{Sr}/^{86}\text{Sr}_i$ values (0.7055 – 0.7120)
383 and ϵNd_i (-1.5 to -5.5). The range in isotopic values broadly overlaps with the range displayed by the
384 Karoo-Ferrar related dyke suites from the Falkland Island (Hole et al., 2016) and KwaZulu Natal (Riley
385 et al., 2006), which overlap in age with the eastern Antarctic Peninsula lava successions (~178 Ma).

386 The Cretaceous dykes from the Black Coast region overlap in composition with the Jason Peninsula
387 basalts and some of the Eland Mountains basalts. However, generally the Sr-Nd data fail to identify a
388 subset of more depleted compositions from the Eland Mountains-Kamenev Nunatak successions
389 that is observed in the trace element data.

390

391 **6. Discussion**

392

393 Weddell Sea rift magmatism during the Early – Middle Jurassic is likely to be related to three
394 broadly contemporaneous magmatic/tectonic processes:

- 395 i) The emplacement of the Ferrar LIP and its potential correlatives in KwaZulu Natal and
396 the Falkland Islands in the interval 183 – 176 Ma.
- 397 ii) The emplacement of the southern Weddell magnetic province (SWMP) at 180 – 175 Ma,
398 which is potentially linked to back-arc basin extension of the Antarctic Peninsula
399 continental margin arc and strike-slip movement along the Pagano shear zone.
- 400 iii) Magmatism associated with the emplacement of the northern Weddell magnetic
401 province (NWMP) after at least 175 Ma and any potential Falkland Islands-KwaZulu Natal
402 link.

403 It is likely that mafic magmas were emplaced in the WSRS during all three of these events (Jordan
404 et al., 2013; Jordan et al., 2017; Leat et al., 2018). While the compositions of the Ferrar magmatism
405 are well known, there are no known outcrops or samples from the magmas forming the two
406 magnetic provinces in the WSRS.

407

408 *6.1 Links to the Ferrar large igneous province*

409

410 Wever and Storey (1992) investigated a broad range of mafic greenstones (Hjort Formation) from
411 the Black Cost region of the eastern Antarctic Peninsula and divided them into three distinct groups.

412 They highlighted that the most isotopically enriched rocks (Group III) of the Black Coast basaltic
413 successions were akin to the low-Ti tholeiites of the Ferrar LIP. However, their interpretation was
414 based on a small sample set with limited geochemical data and no geochronological control. The age
415 data and geochemistry interpreted here and presented in Riley et al. (2016) also make it tempting to
416 suggest a potential correlation between the eastern Antarctic Peninsula successions and the Ferrar
417 LIP as geochemical characteristics of part of the Eland Mountains-Kamenev Nunatak successions
418 overlap with the dominant Mount Fazio chemical rock type of the Ferrar LIP (Fig. 6). Also, the
419 presence of magnetic anomalies in the southern Weddell Sea are consistent with mafic-intermediate
420 sills or lavas (Jordan et al., 2017) and could partly represent an extension of the Ferrar LIP toward
421 the Antarctic Peninsula margin.

422 Although the age of the Eland Mountains-Kamenev Nunatak (Black Coast) successions, at 180 –
423 177 Ma, is ~3 – 6 Myr younger than the main phase of Ferrar LIP magmatism (Burgess et al., 2015),
424 the Black Coast basalts could represent the final phase of magmatism on the periphery of a more
425 extensive province. The pre-breakup reconstruction of Gondwana at 180 Ma (Fig. 2) places the Black
426 Coast region an equivalent distance from the proposed plume centre as the Transantarctic
427 Mountains. The long-distance transport of Ferrar magmas described by Leat (2008) indicates that
428 extension of the Ferrar LIP into the Black Coast region is potentially feasible. The caveat to any Ferrar
429 LIP-Black Coast association is that although there is good geochemical agreement between some
430 eastern Antarctic Peninsula basaltic successions, overwhelmingly there are clear geochemical
431 differences to the more depleted units from Eland Mountains-Kamenev Nunatak, Hjort Formation
432 and Sweeney Formation (Riley et al., 2016). Although the thicker successions (~800 m) at Eland
433 Mountains-Kamenev Nunatak are the most likely candidates for any Antarctic Peninsula expression
434 of the Ferrar LIP, an age discrepancy of ~5 Myr between the Ferrar LIP (183 ± 1 Ma; Burgess et al.,
435 2015) and the Eland Mountains succession (178 ± 2 Ma; Riley et al., 2016), combined with a depleted
436 geochemical signature for the main part of the succession is considered to make such a correlation
437 unlikely.

438 Other potential distal correlatives of the Ferrar LIP include basaltic/dolerite dyke swarms that
439 crop out in KwaZulu Natal in southern Africa (Riley et al., 2006) and the Falkland Islands (Hole et al.,
440 2016). Both Riley et al. (2006) and Hole et al. (2016) dated the dyke swarms in the interval 182 – 176
441 Ma and suggested the compositions were transitional between Karoo and Ferrar LIP magma types,
442 and akin to those of the Theron Mountains of Antarctica (Fig. 1; Brewer et al., 1992). Pre-breakup
443 reconstructions of Gondwana at 180 Ma place the Falkland Islands, KwaZulu Natal and the Theron
444 Mountains in adjacent locations at the junction of the Karoo and Ferrar LIPs (Fig. 2). Extrapolating
445 this association to include the eastern Antarctic Peninsula basaltic successions, despite some overlap
446 in chronology (with Falkland Islands and KwaZulu Natal) is however, tectonically unlikely and not
447 supported by the geochemistry. Hence, a direct correlation between Early Jurassic Antarctic
448 Peninsula basaltic magmatism and the Ferrar LIP (including KwaZulu Natal-Falkland Islands) is not
449 supported.

450

451 *6.2 Association with the Southern Weddell magnetic province (SWMP)*

452

453 The magnetic anomalies of the SWMP are less magnetic than the anomalies of the NWMP and
454 are interpreted to represent a mix of mafic and intermediate-silicic intrusions or lavas (Jordan et al.,
455 2017). The SWMP anomalies trend NW-SE and Jordan et al. (2017) suggested they relate to broadly
456 east-west rifting in a back-arc basin setting of the Antarctic Peninsula. Back-arc extension has been
457 indirectly dated at ~175 Ma based on the dating of granitoid bodies (Leat et al., 2018) emplaced into
458 the active Pagano shear zone of the Ellsworth Mountains (Fig. 3b). Movement along the Pagano
459 shear zone accommodated motion associated with the back-arc extension, hence the
460 contemporaneous emplacement and deformation of the Pagano Nunatak shear zone granite (174.62
461 \pm 0.16 Ma; Craddock et al., 2017) dates a period of major extension.

462 The basaltic successions from Eland Mountains-Kamenev Nunatak have an age essentially
463 coincident with extension (178 \pm 2 Ma; Riley et al., 2016) and geochemical characteristics that are

464 consistent with a transition from arc-related basalts to back-arc basin basalts from a deeper, more
465 depleted source. Magmatism of this developing back-arc basin, related to east-west extension is
466 preserved in minor north-south magnetic anomalies identified close to the Antarctic Peninsula
467 margin (McGibbon and Wever (1991), Ferris et al., 2002) and also by the magnetic fabric of the
468 SWMP, although this has been largely overprinted by the later NWMP adjacent to the Black Coast
469 (Fig. 3b). The basaltic successions from the eastern Antarctic Peninsula lack a clear 'arc' affinity that
470 is typical of other basaltic successions of the Antarctic Peninsula (Leat et al., 2002) and are also
471 distinct in their greater thickness (~800 m) and field characteristics (multiple, amygdaloidal flow
472 units). The Eland Mountains-Kamenev Nunatak successions have a stratigraphically lower age of
473 180.2 ± 0.7 Ma and an upper age of 177.6 ± 1.0 Ma and geochemically record the transition to true
474 back-arc basin basalts. An Early Jurassic back-arc basin setting is also supported by facies analysis of
475 >4 km thickness of sedimentary rocks of the Latady Group, which were deposited in the developing
476 Latady Basin (Hunter and Cantrill, 2006).

477 The interpretation of geophysical data from the Falkland Plateau (Schimschal and Jokat, 2019)
478 indicates that the Falkland Plateau basin consists of up to 20 km of thick oceanic crust, which is
479 related to an extensional back-arc setting. In their model, Schimschal and Jokat (2019) suggest rifting
480 was initiated at ~178 Ma after the emplacement of the Karoo-Ferrar dyke swarms on the Falkland
481 Islands (Hole et al., 2016).

482 Therefore, several lines of evidence strongly point to an extensional back-arc regime at ~178 Ma
483 in the proto-Weddell Sea; a tectonic setting which marked the initial phase of Weddell Sea opening
484 and one of the earliest phases of Gondwana breakup. The tectonic interpretations of Jordan et al.
485 (2017) and Schimschal and Jokat (2019) both indicate that east-west extension was underway at
486 ~178 Ma, whilst onshore magmatism described by McGibbon and Wever (1991), Wever and Storey
487 (1992), Riley et al. (2016) and this study also indicate rift-related magmatism at ~178 Ma.

488 Geochemically, the back-arc basin basalts of the Eland Mountains-Kamenev Nunatak successions
489 show a source that changed from an arc-influenced setting to a more depleted, asthenospheric-like

490 source as the back-arc basin developed. This transition occurred in the interval 180 – 177 Ma and
491 likely reflects the early stages of back-arc basin development and the onset of east-west extension in
492 the adjacent Weddell Sea. Back-arc related extension continued until at least ~175 Ma based on the
493 age of the Pagano Nunatak granite and was likely to have ceased at the time of onset of extensive
494 silicic volcanism at ~171 Ma.

495 It is also significant that the SWMP is less magnetic than the NWMP (Jordan et al., 2017) and
496 likely reflects a mix of mafic-intermediate lavas which is consistent with the successions identified on
497 the Black Coast (Wever and Storey, 1992; McGibbon and Wever, 1991; Riley et al., 2016). The coast
498 parallel magnetic anomalies of the SWMP are no longer clearly preserved adjacent to the Black
499 Coast, as they have been overprinted by the later stage NWMP (Fig. 4). However, N-S magnetic
500 trends identified by Ferris et al., 2002 in the black coat region could reflect back arc extension.

501

502 *6.3 Association with the Northern Weddell magnetic province (NWMP)*

503

504 The Northern Weddell magnetic province (NWMP) is a complex array of lineations with a
505 dominant NE-SW trend (Fig. 3b) attributed to extensional tectonics (Jokat and Herter, 2016; Jordan
506 et al., 2017). The magnetic anomalies of the NWMP are adjacent to the Eland Mountains-Kamenev
507 Nunatak basaltic successions (Fig. 3b) and the magnetic anomalies are interpreted to represent
508 mafic intrusions/lavas that were the precursor to the onset of seafloor spreading in the Weddell Sea.
509 The NWMP extension postdated the SWMP but was possibly coincident with the later separation of
510 the Falkland Plateau from the Weddell Sea rift region (Ferris et al., 2000).

511 If the Eland Mountains-Kamenev Nunatak basaltic successions do represent an onshore
512 expression of the magmatism associated with extension of the NWMP then the timing is critical.
513 Extension in the NWMP has been interpreted by Jordan et al. (2017) to have likely taken place after
514 extension in the SWMP at ~178 Ma. However, given that movement on the Pagano Shear Zone was
515 still ongoing at ~175 Ma, which is linked to the emplacement of the SWMP, it implies that extension

516 in the NWMP must postdate 175 Ma. There is no geochemical control on the offshore magmatism
517 associated with the NWMP to correlate with the basaltic successions from Eland Mountains-
518 Kamenev Nunatak. The identification of north-south trending magnetic anomalies by McGibbon and
519 Wever (1991) that are likely to reflect an extension of the Eland Mountains-Kamenev Nunatak
520 succession indicate that an association with the NE-SW trending magnetic anomalies of the NWMP is
521 unlikely even though they are adjacent in present day configurations.

522 Jordan et al. (2017) also suggested that the NWMP could represent a transtensional setting
523 associated with a later stage Gondwana configuration, in which case the eastern Antarctic Peninsula
524 basalts would very likely predate such a tectonic setting and make any association with the NWMP
525 unlikely. Also, the NWMP is characterized by more strongly magnetic anomalies indicating mafic
526 intrusions, unlike the mafic-intermediate compositions of the Black Coast successions.

527 In summary, the chronology of events make any association between the Black Coast basaltic
528 successions and the NWMP unlikely on the basis that the NWMP postdates the emplacement of the
529 SWMP and that the basaltic successions are related to an extensional regime that continued until
530 ~175 Ma.

531

532 **7. Conclusions**

533

534 - The Weddell Sea rift system has developed on continental lithosphere and is underlain by
535 extensive mafic lavas and/or intrusions that have been attributed to rift-related magmatism
536 or a continuation of the Ferrar LIP into the proto Weddell Sea (Jordan et al., 2017).

537

538 - A thick (~800 m) succession of basaltic-basaltic andesite lavas from the eastern Antarctic
539 Peninsula are adjacent to the Weddell Sea margin and provide a rare onshore example of
540 magmatism related to the tectonic history of the Weddell Sea.

541

- 542 - The lava successions were emplaced into a developing back-arc extensional setting in the
543 interval 180 – 177 Ma and exhibit a trend from arc-like basalts of a continental margin
544 setting to a more depleted, deeper-seated source, typical of back-arc basin basalts.
545
- 546 - Offshore magnetic anomalies have been attributed to east-west extension dated at ~175 Ma
547 and are interpreted to have developed in a back-arc extensional setting.
548
- 549 - Further evidence for back-arc related magmatism at ~178 Ma is interpreted from the
550 Falkland Plateau region (Schimschal and Jokat, 2019). The first phase of Weddell Sea
551 extension and rifting is therefore related to Early Jurassic back-arc extension along the
552 Antarctic Peninsula continental margin associated with recognized Early Jurassic subduction
553 (Riley et al., 2017). Any potential correlation between the basaltic successions of the Black
554 Coast and the extensive basaltic lavas and sills of the Ferrar large igneous province are
555 discounted on the basis of a ~5 Myr age discrepancy and geochemical differences.
556

557 **Acknowledgements**

558 This study is part of the British Antarctic Survey Polar Science for Planet Earth programme, funded by
559 the Natural Environmental Research Council. The field and air operations staff at Rothera Research
560 Station in Antarctica are thanked for their support. This paper has benefited from the thoughtful
561 reviews of Ian Dalziel and Wilfried Jokat.
562

563 **References**

564

565 Adie R. J., 1952. The position of the Falkland Island in a reconstruction of Gondwanaland. *Geological*
566 *Magazine* 89, 401–410.

567 Barker, P.F., 2001. Scotia Sea regional tectonic evolution: implications for mantle flow and paleo-
568 circulation. *Earth Science Reviews* 55, 1-39.

569 Brewer, T. S., Hergt, J. M., Hawkesworth, C. J., Rex, D. & Storey, B. C., 1992. Coats Land dolerites and
570 the generation of Antarctic continental flood basalts. In: Storey, B., Alabaster, T. & Pankhurst, R.
571 (eds) *Magmatism and the Causes of Continental Break-up*. Geological Society, London, *Special*
572 *Publication* 68, 185–208.

573 Burgess, S.D., Bowring, S.A., Fleming, T.H., Elliot, D.H., 2015. High-precision geochronology links the
574 Ferrar large igneous province with early-Jurassic ocean anoxia and biotic crisis. *Earth and*
575 *Planetary Science Letters* 415, 90-99.

576 Burton-Johnson, A., Riley, T.R., 2015. Autochthonous vs. accreted terrane development of
577 continental margins: A new in situ tectonic history of the Antarctic Peninsula. *Journal of the*
578 *Geological Society, London*, doi:10.1144/jgs2014-110.

579 Craddock, J.P., Schmitz, M.D, Crowley, J.L., Larocque, J., Pankhurst, R.J., Juda, N., Konstantinou, A.,
580 Storey, B., 2017. Precise U-Pb zircon ages and geochemistry of Jurassic granites, Ellsworth-
581 Whitmore terrane, central Antarctica. *Geological Society of America Bulletin* 129, 118-136.

582 Curtis, M.L., Storey, B.C., 1996. A review of geological constraints on the pre-break-up position of the
583 Ellsworth Mountains within Gondwana: implications for Weddell Sea evolution, in: Storey, B.C.,
584 King, E.C., Livermore, R.A. (Eds.), *Weddell Sea Tectonics and Gondwana Break-up*. Geological
585 Society, London, *Special Publications* 108, 11-30.

586 Dalziel, I.W.D, Elliot, D.H., 1982. West Antarctica: Problem child of Gondwanaland. *Tectonics*, 1, 3-
587 19.

588 Dalziel, I.W.D., 2013. Antarctica and supercontinental evolution: clues and puzzles. *Earth and*
589 *Environmental Science Transactions of the Royal Society of Edinburgh* 104, 3–16.

590 Elliot, D.H., Fleming, T.H., Kyle, P.R., Foland, K.A., 1999. Long-distance transport of magmas in the
591 Jurassic Ferrar large igneous province, Antarctica. *Earth and Planetary Science Letters* 167, 89-
592 104.

593 Elliot, D.H., Fleming, T.H., 2000. Weddell triple junction: The principal focus of Ferrar and Karoo
594 magmatism during initial breakup of Gondwana. *Geology* 28, 539-542.

595 Ferris, J.K., Johnson, A.C., Storey, B.C., 1998. Form and extent of the Dufek intrusion, Antarctica,
596 from newly compiled aeromagnetic data. *Earth and Planetary Science Letters* 154, 185-202.

597 Ferris, J.K., Vaughan, A.P.M., Storey, B.C., 2000. Relics of a complex triple junction in the Weddell
598 Sea embayment, Antarctica. *Earth and Planetary Science Letters* 178, 215-230.

599 Ferris, J.K., Vaughan, A.P.M., King, E.C., 2002. A window on West Antarctic crustal boundaries: the
600 junction between the Antarctic Peninsula, The Filchner Block, and the Weddell Sea oceanic
601 lithosphere. *Tectonophysics* 347, 13-23.

602 Fleming, T. H., Foland, K. A. & Elliot, D. H., 1995. Isotopic and chemical constraints on the crustal
603 evolution and source signature of Ferrar magmas, north Victoria Land, Antarctica. *Contributions*
604 *to Mineralogy and Petrology* 121, 217–236.

605 Fleming, T.H., Heimann, A., Foland, K.A., Elliot, D.H., 1997. $^{40}\text{Ar}/^{39}\text{Ar}$ geochronology of Ferrar dolerite
606 sills from the Transantarctic Mountains, Antarctica: implications for the age and origin of the
607 Ferrar magmatic province. *Geological Society of America, Bulletin* 109, 533-546.

608 Grunow, A.M., Kent, D.V., Dalziel, I.W.D., 1987. Mesozoic evolution of West Antarctica and the
609 Weddell Sea basin: new paleomagnetic constraints. *Earth and Planetary Science Letters* 86, 16-
610 26.

611 Hergt, J.M., Brauns, C.M., 2001. On the origin of Tasmanian dolerites. *Australian Journal of Earth*
612 *Sciences* 48, 543-549.

613 Hole, M.J., Ellam, R.M., Macdonald, D.I.M., Kelley, S.P., 2016. Gondwana break-up related
614 magmatism in the Falkland Islands. *Journal of the Geological Society, London* 173, 108-126.

615 Hunter, M.A., Cantrill, D.J., 2006. A new stratigraphy for the Latady Basin, Antarctic Peninsula: Part 2.
616 Latady Group and basin evolution. *Geological Magazine* 143, 797-819.

617 Hunter, M.A., Cantrill, D.J., Flowerdew, M.J., Millar, I.L., 2005. Middle Jurassic age for the Botany Bay
618 Group: implications for Weddell Sea Basin creation and southern hemisphere biostratigraphy.
619 Journal of the Geological Society of London 162, 745-748.

620 Jokat, W., Herter, U., 2016. Jurassic failed rift system below the Filchner-Ronne-Shelf, Antarctica:
621 New evidence from geophysical data. Tectonophysics 688, 65-83.

622 Jordan, T. A., Ferraccioli, F., Ross, N., Siegert, M.J., Corr. H.F., Leat, P.T., Bingham, R.G., Rippin, D.M.,
623 2013. Structure and inland extent of the Mesozoic Weddell Sea Rift, Antarctica, imaged by new
624 aerogeophysical data. Tectonophysics 585, 137-160.

625 Jordan, T.A., Ferraccioli, F., Leat, P.T., 2017. A new model for microplate movement, magmatism,
626 and distributed extension in the Weddell Sea Rift System of West Antarctica. Gondwana Research
627 42, 29-48.

628 Jourdan, F., Féraud, G., Bertrand, H., Watkeys, M.K., 2007. From flood basalts to the inception of
629 oceanization: example from the $^{40}\text{Ar}/^{39}\text{Ar}$ high-resolution picture of the Karoo large igneous
630 province. Geochemistry, Geophysics, Geosystems 8.

631 King, E.C., 2000. The crustal structure and sedimentation of the Weddell Sea embayment:
632 implications for Gondwana reconstructions. Tectonophysics 327, 195-212.

633 König, M., Jokat, W., 2006. The Mesozoic breakup of the Weddell Sea. Journal of Geophysical
634 Research - Solid Earth 111, 1–28.

635 Leat P.T., 2008. On the long-distance transport of Ferrar magmas. In: Thomson, K., Petford, N. (Eds.),
636 Structure and emplacement of high-level magmatic systems. Geological Society of London Special
637 Publication 302, 45-61.

638 Leat, P.T., Riley, T.R., Wareham, C.D., Millar, I.L., Kelley, S.P., Storey, B.C., 2002. Tectonic setting of
639 primitive magmas in volcanic arcs: an example from the Antarctic Peninsula. Journal of the
640 Geological Society, London 159, 31-44.

641 Leat, P.T., Jordan T. A., Flowerdew, M. J., Riley, T.R., Ferraccioli, F. & Whitehouse, M.J. 2018. Jurassic
642 High Heat Production granites associated with the Weddell rift system, Antarctica.
643 Tectonophysics, 722, 249-264.

644 Lee, H.M., Lee, J.I., Lee, M.J., Kim, J., Choi, S.W., 2012. The A-type Pirrit Hills granite, West Antarctica
645 an example of magmatism associated with the Mesozoic break-up of the Gondwana
646 supercontinent. Geosci. J. 16, 421–433.

647 Leitchenkov, G.L., Kudryavtzev, G.A., 1997. Structure and origin of the Earth's Crust in the Weddell
648 Sea Embayment (beneath the front of the Filchner and Ronne ice shelves) from deep seismic
649 sounding data. Polarforschung 67, 143–154.

650 Martin, A.K., 2007. Gondwana breakup via double-saloon-door rifting and seafloor spreading in a
651 backarc basin during subduction rollback. Tectonophysics, 445, 245-272.

652 McGibbon, K.J., Garrett, S.W., 1987. Magnetic anomalies over the Black Coast, Palmer Land. British
653 Antarctic Survey Bulletin 76, 7-20.

654 McGibbon, K.J., Wever, H.E., 1991. Magnetic evidence for gabbroic plutons in the Black Coast area,
655 Palmer Land. In: Thomson, M.R.A., Crame, J.A., Thomson, J.W. (eds), Geological evolution of
656 Antarctica. Cambridge University press, Cambridge, 395-398.

657 Minor, D. R. & Mukasa, S. B. (1997). Zircon U-Pb and hornblende ^{40}Ar - ^{39}Ar ages for the Dufek layered
658 mafic intrusion, Antarctica: Implications for the age of the Ferrar large igneous province.
659 Geochimica et Cosmochimica Acta 61, 2497-2504.

660 Molzahn, M., Reisberg, L., Wörner, G., 1996. Os, Sr, Nd, Pb and O isotope and trace element data
661 from the Ferrar flood basalts, Antarctica: evidence for an enriched subcontinental lithospheric
662 source. Earth and Planetary Science Letters 144, 529-546.

663 Mortimer, N., Parkinson, D., Raine, J.I., Adams, C.J., Graham, I.J., Oliver, P.J., Palmer K. 1995. Ferrar
664 magmatic province rocks discovered in New Zealand: Implications for Mesozoic Gondwana
665 geology. Geology 23, 185-188.

666 Mueller, C.O, Jokat, W., 2019. The initial Gondwana break-up: A synthesis based on new potential
667 field data of the Africa-Antarctica Corridor. *Tectonophysics* 750, 301-328.

668 Pankhurst, R.J., Riley, T.R., Fanning, C.M., Kelley, S.P., 2000. Episodic silicic volcanism in Patagonia
669 and the Antarctic Peninsula: chronology of magmatism associated with break-up of Gondwana.
670 *Journal of Petrology* 41, 605-625.

671 Pearce, J.A., Stern, R.J., 2006. Origin of back-arc basin magmas: trace element and isotope
672 perspectives. In: *Back-arc spreading systems: geological, biological, chemical and physical*
673 *interactions. Geophysical Monograph Series, 166, 63-86.*

674 Randall, D.E., MacNiocaill, C., 2004. Cambrian palaeomagnetic data confirm a Natal Embayment
675 location for the Ellsworth-Whitmore Mountains, Antarctica, in Gondwana reconstructions:
676 *Geophysical Journal International* 157, 105-116.

677 Riley, T.R., Leat, P.T., 1999. Large volume silicic volcanism along the proto-Pacific margin of
678 Gondwana: lithological and stratigraphical investigations from the Antarctic Peninsula. *Geological*
679 *Magazine* 136, 1-16.

680 Riley, T.R., Knight, K.B., 2001. Age of pre-break-up Gondwana magmatism: a review. *Antarctic*
681 *Science* 13, 99-110.

682 Riley, T.R., Leat, P.T., Kelley, S.P., Millar, I.L., Thirlwall, M.F., 2003. Thinning of the Antarctic Peninsula
683 lithosphere through the Mesozoic: evidence from Middle Jurassic basaltic lavas. *Lithos* 67, 163-
684 179.

685 Riley, T.R., Leat, P.T., Curtis, M.L., Millar, I.L., Fazel, A., 2005. Early-Middle Jurassic Dolerite Dykes
686 from Western Dronning Maud Land (Antarctica): Identifying Mantle Sources in the Karoo Large
687 Igneous Province. *Journal of Petrology* 46, 1489-1524.

688 Riley, T.R., Curtis, M.L., Leat, P.T., Watkeys, M.K., Duncan, R.A., Millar, I.L., Owens, W.H., 2006.
689 Overlap of Karoo and Ferrar magma types in the KwaZulu-Natal region of South Africa. *Journal of*
690 *Petrology* 47, 541-566.

691 Riley, T.R., Flowerdew, M.J., Hunter, M.A., Whitehouse, M.J. (2010). Middle Jurassic rhyolite volcanism of
692 eastern Graham Land, Antarctic Peninsula: age correlations and stratigraphic relationships. *Geological*
693 *Magazine*, 147, 581-595.

694 Riley, T.R., Curtis, M.L., Flowerdew, M.J. & Whitehouse, M.J., 2016. Evolution of the Antarctic
695 Peninsula lithosphere: evidence from Mesozoic mafic rocks. *Lithos* 244, 59-73.

696 Riley, T.R., Flowerdew, M.J., Pankhurst, R.J., Curtis, M.L., Millar, I.L., Fanning, C.M., Whitehouse, M.J.,
697 2017. Early Jurassic subduction-related magmatism on the Antarctic Peninsula and potential
698 correlation with the Subcordilleran plutonic belt of Patagonia. *Journal of the Geological Society*,
699 London, 174, 365-376.

700 Schimschal, C.M., Jokat, W., 2019. The Falkland Plateau in the context of Gondwana breakup.
701 *Gondwana Research* 68, 108-115.

702 Schopf, J.M., 1969. Ellsworth Mountains: Position in West Antarctica due to sea-floor spreading.
703 *Science*, 164, 63-66.

704 Storey, B.C., Dalziel, I.W.D., Garrett, S.W., Grunow, A., Pankhurst, R.J., Vennum, W., 1988. West
705 Antarctica in Gondwanaland: crustal blocks, reconstruction and breakup processes.
706 *Tectonophysics* 155, 381–390.

707 Storey, B.C., Vaughan, A.P.M. & Millar, I.L. 1996. Geodynamic evolution of the Antarctic Peninsula
708 during Mesozoic times and its bearing on Weddell Sea history. *Geological Society of London*,
709 *Special Publication*, No. 108, 87-103.

710 Studinger, M., Miller, H., 1999. Crustal structure of the Filchner-Ronne shelf and Coats Land,
711 Antarctica, from gravity and magnetic data: implications for the breakup of Gondwana. *Journal of*
712 *Geophysical Research - Earth Surface* 104, 20379–20394.

713 Suárez, M., 1976. Plate tectonic model for southern Antarctic Peninsula and its relation to southern
714 Andes. *Geology* 4, 211–214.

715 Svensen, H., Corfu, F., Polteau, S., Hammer, O., Planke, S., 2012. Rapid magma emplacement in the
716 Karoo large igneous province. *Earth and Planetary Science Letters* 325-326, 1-9.

717 Vaughan, A.P.M., Storey, B.C., 2000. The eastern Palmer Land shear zone: a new terrane accretion
718 model for the Mesozoic development of the Antarctic Peninsula. *Journal of the Geological*
719 *Society, London* 157, 1243–1256.

720 Vaughan, A.P.M., Pankhurst, R.J., Fanning, C.M., 2002. A mid-Cretaceous age for the Palmer Land
721 event: implications for terrane accretion timing and Gondwana palaeolatitudes. *Journal of the*
722 *Geological Society, London* 159, 113-116.

723 Vaughan, A.P.M., Leat, P.T., Dean, A.A., Millar, I.L., 2012. Crustal thickening along the West Antarctic
724 Gondwana margin during mid-Cretaceous deformation of the Triassic intra-oceanic Dyer Arc.
725 *Lithos* 142-143, 130–147.

726 Veevers, J.J., 2012. Reconstructions before rifting and drifting reveal the geological connections
727 between Antarctica and its conjugates in Gondwanaland. *Earth Science Reviews* 111, 249-318.

728 Wever, H.E., Storey, B.C., 1992. Bimodal magmatism in northeast Palmer Land, Antarctic Peninsula:
729 geochemical evidence for a Jurassic ensialic back-arc basin. *Tectonophysics* 205, 239–259.

730 Zundel, M., Spiegel, C., Mehling, A., Lisker, F., Hillenbrand, C.-D, Monien, P., Klugel, A., 2019.
731 Thurston Island (West Antarctica) between Gondwana subduction and continental separation: a
732 multistage evolution revealed by apatite thermochronology. *Tectonics* 38, 1-20.

733

734 **List of figures**

735

736 Figure 1: Map of Antarctica showing the key localities in the Weddell Sea sector of Antarctica. JP;
737 Jason Peninsula; EM: Eland Mountains; KN: Kamenev Nunatak; LP: Leining Peak; HN: Haag
738 Nunataks; EWM: Ellsworth-Whitmore Mountains; FRIS: Filchner-Ronne Ice Shelf; BI: Berkner Island.

739

740 Figure 2: Regional Gondwana reconstruction at 180 Ma from Jordan et al. (2017). The pre-breakup
741 positions of the Haag Nunataks-Ellsworth Whitmore Mountains blocks are shown adjacent to the
742 Falkland Islands block in the Natal Embayment. AP: Antarctic Peninsula; FI: Falkland Islands; TI:
743 Thurston Island; NE: Natal Embayment; MBL: Marie Byrd Land; KZN: KwaZulu Natal; Tas: Tasmania.
744 This reconstruction is adapted from Jordan et al. (2017) and Jokat and Herter (2016) and the proto-
745 Pacific margin configuration of crustal blocks cannot be considered definitive.

746

747 Figure 3: Aeromagnetic data and identified structural trends across the Weddell Sea Rift System
748 (Jordan et al., 2017). a) Aeromagnetic data compilation. b) Inferred magnetic lineations from the
749 aeromagnetic data highlighting the distinct trend of the NWMP and SWMP regions. The sub-ice
750 magnetic lineations of McGibbon and Garrett (1987) are shown along the Black Coast. AP: Antarctic
751 Peninsula; OA: Orion Anomaly; EA: Explora Anomaly; FR: Filchner Rift; DI: Dufek Intrusion; PSZ:
752 Pagano shear zone; EWM: Ellsworth-Whitmore Mountains.

753

754 Figure 4: Schematic diagram illustrating the proposed two-phase development of the NWMP and
755 SWMP (Jordan et al. (2017). a) Back-arc extension at ~178 Ma led to the development of the N-S
756 oriented structures of the SWMP. The onshore expression of back-arc magmatism is highlighted by
757 the star on the Black Coast. Movement associated with back-arc extension was accommodated along
758 the Pagano shear zone (PSZ). b) Development of the NWMP took place after 174 Ma and was
759 associated with broadly N-S extension associated with the breakup of East Antarctica and Africa.

760

761 Figure 5: Weakly deformed amygdaloidal basalts from the Eland Mountains. N10.123.1 [70.6653 S,
762 062.7750 W].

763

764 Figure 6: Variations in Th/Yb vs. Nb/Yb for mafic rocks from the eastern Antarctic Peninsula relative
765 to the MORB-OIB array (Pearce and Peate, 1995). The Eland Mountains-Kamenev Nunatak analyses
766 are from Riley et al. (2016), Hjort Formation (Wever and Storey, 1992), Jason Peninsula (Riley et al.,
767 2003). Cretaceous dykes from the Black Coast represent arc-modified lithosphere of the eastern
768 Antarctic Peninsula (Leat et al., 2002). Average Ferrar MFCT (Mount Fazio chemical type) is from
769 Molzahn et al. (1996).

770

771 Figure 7: Plot of Ba/Nb vs. Th/Nb to investigate the relative roles of shallow and deep subduction
772 components in a back-arc extensional setting (Pearce and Stern, 2006). Ba/Nb is the proxy for total
773 subduction input and Th/Nb represents the proxy for deep subduction input. The deep component is
774 highlighted by the diagonal vector and the shallow component is a vertical vector. Back-arc basin
775 basalts will follow the deep component vector (e.g. Eland Mountains and Sweeney Formation
776 basalts; Riley et al., 2016; Hunter et al., 2006) and the continental margin arc basalts will follow the
777 vertical vector (e.g. Cretaceous Black Coast basalts; Leat et al., 2002).

778

779 Figure 8: Chondrite (Nakamura, 1974) normalized REE diagrams for the basaltic successions from the
780 east coast of the Antarctic Peninsula. Light REE enriched abundances from Jason Peninsula (Riley et
781 al., 2003) and the Cretaceous Black Coast dykes (Leat et al., 2002) are shown relative to the more
782 depleted compositions from the Sweeney Formation (shaded area; Hunter et al., 2006) and the
783 Eland Mountains succession (line data; Riley et al., 2016).

784

785 Figure 9: $^{87}\text{Sr}/^{86}\text{Sr}_i$ vs. ϵNd_i for magmatic rocks from the eastern Antarctic Peninsula, shown in
786 comparison to data fields from the Ferrar LIP, Falkland Islands (Hole et al., 2017). KwaZulu Natal
787 (Riley et al., 2006). Data sources: Eland Mountains-Kamenev Nunatak (Wever and Storey, 1992; this
788 study); Sweeney Formation (Hunter et al. 2006); Jason Peninsula (Riley et al. 2003); Cretaceous Black
789 Coast dykes (Leat et al. 2002); Karoo (Riley et al., 2005). KZN: KwaZulu Natal; PST: Port Sussex type;
790 DIT: Dyke Island type; MFCT: Mount Fazio chemical type.
791

Table 1: Sr-Nd isotope geochemistry

Sample	Location	Age	Sm	Nd	$^{147}\text{Sm}/^{144}\text{Nd}$	$^{143}\text{Nd}/^{144}\text{Nd}$	$^{143}\text{Nd}/^{144}\text{Nd}_i$	eps(Nd)	Rb	Sr	$^{87}\text{Rb}/^{86}\text{Sr}$	$^{87}\text{Sr}/^{86}\text{Sr}$	$^{87}\text{Sr}/^{86}\text{Sr}_i$
N10.227.1	Leininger Peak	178	4.90	18.55	0.1596	0.512485	0.512297	-2.1	79.6	50.8	4.54	0.716883	0.70545
N10.436.3	Leininger Peak	178	4.57	21.39	0.1292	0.512392	0.512240	-3.2	76.6	189.9	1.17	0.709828	0.70689
N10.6.1	Eland Mountains	178	3.48	12.93	0.1625	0.512520	0.512329	-1.5	13.9	368.4	0.11	0.707434	0.70716
R.4144.5	Kamenev Nunatak	178	3.83	16.62	0.1393	0.512289	0.512125	-5.5	39.3	137.6	0.83	0.714025	0.71194
R.4291.2	Hjort Fm (III)	178	4.01	15.06	0.1609	0.512347	0.512154	-5.0	35	149	0.68	0.710752	0.70904

Rb-Sr and Sm-Nd isotope analyses were performed at NIGL, Keyworth, UK.

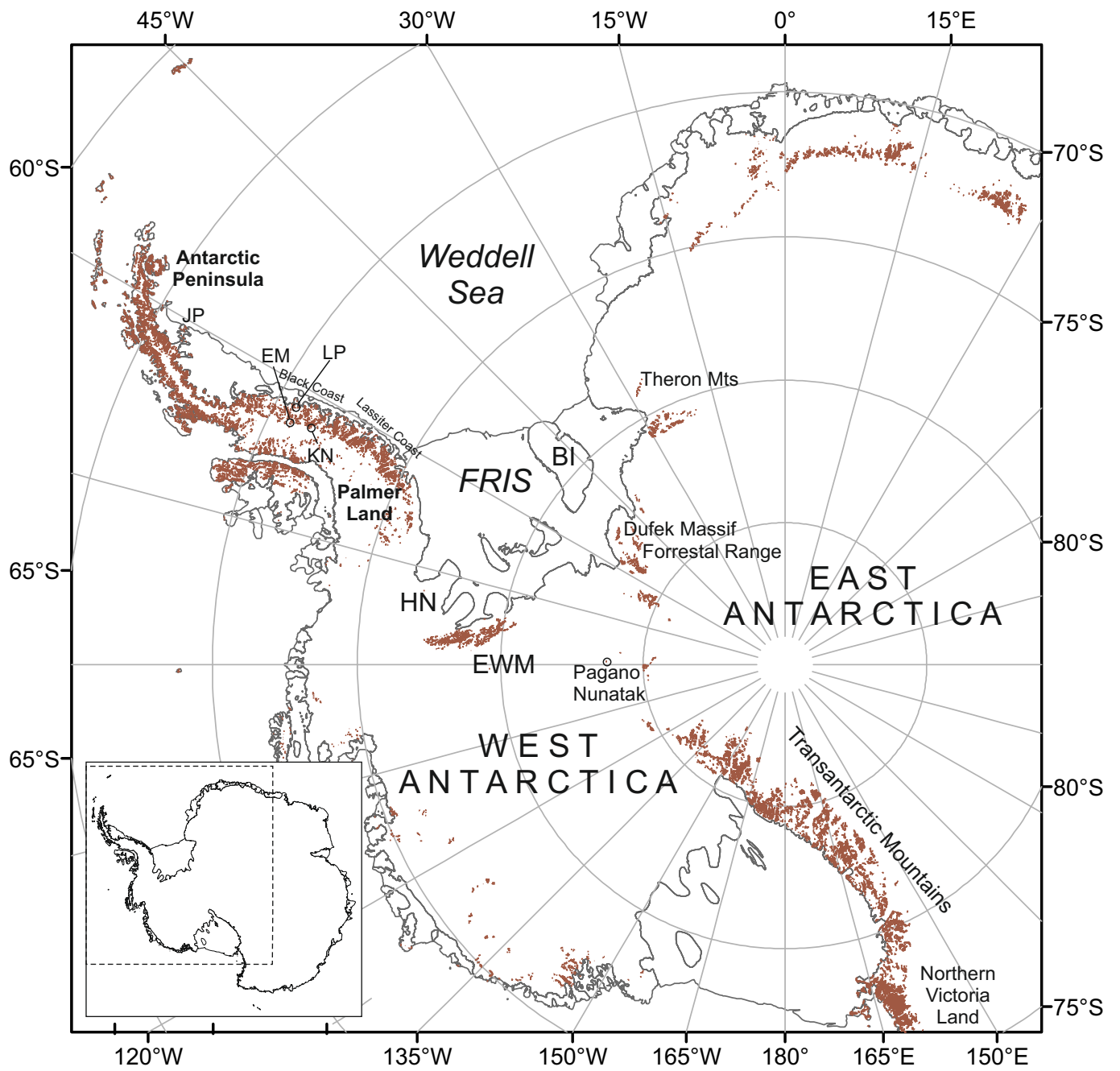


Figure 1

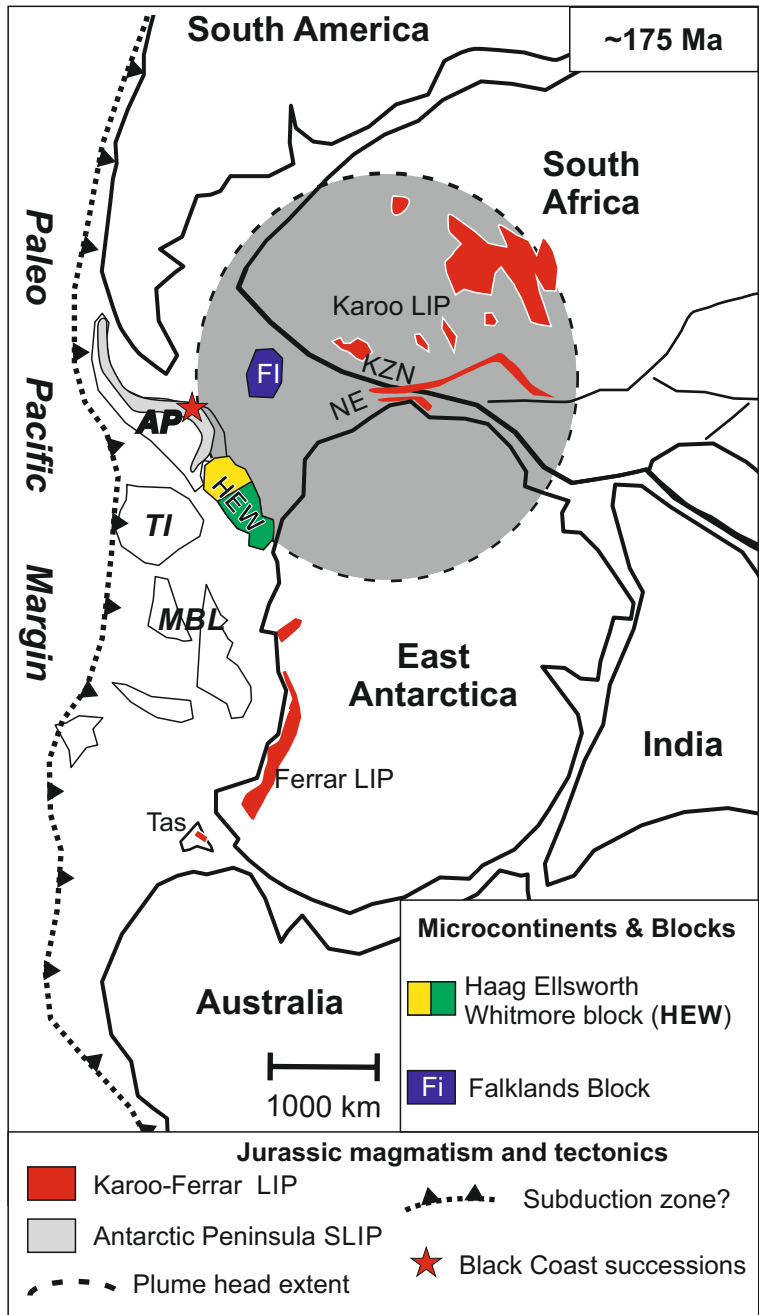


Figure 2

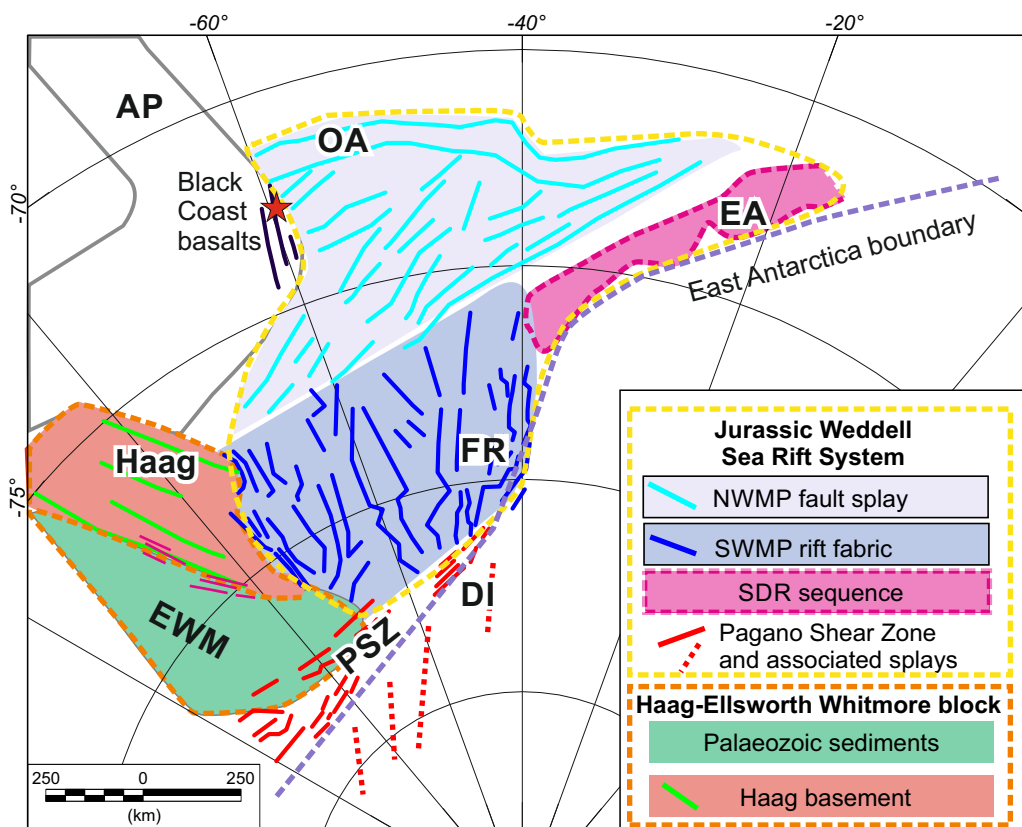
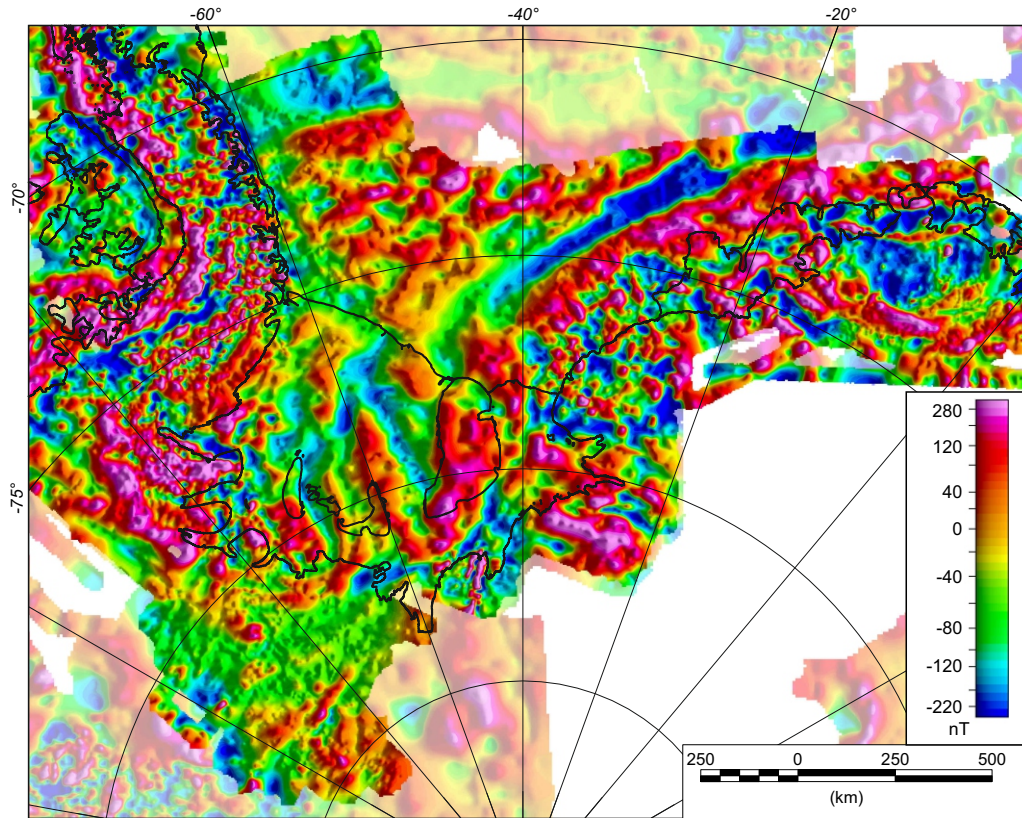


Figure 3

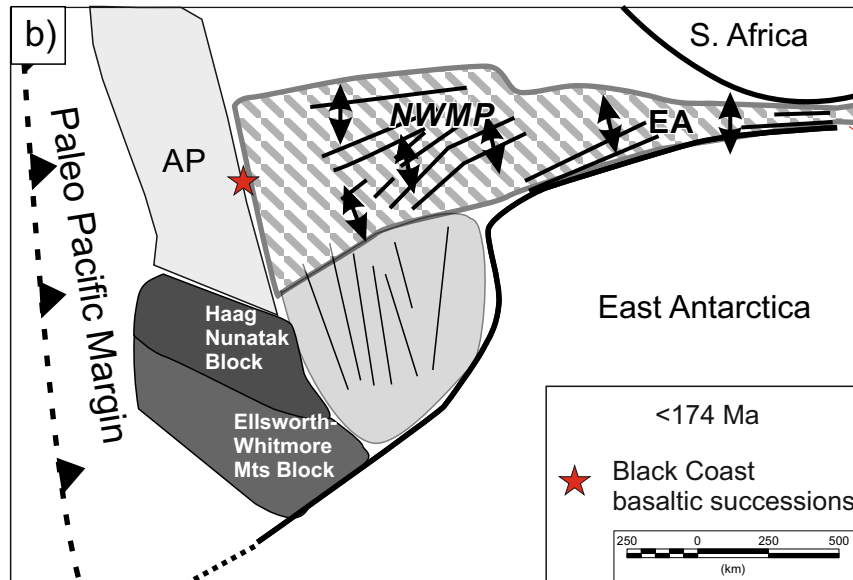
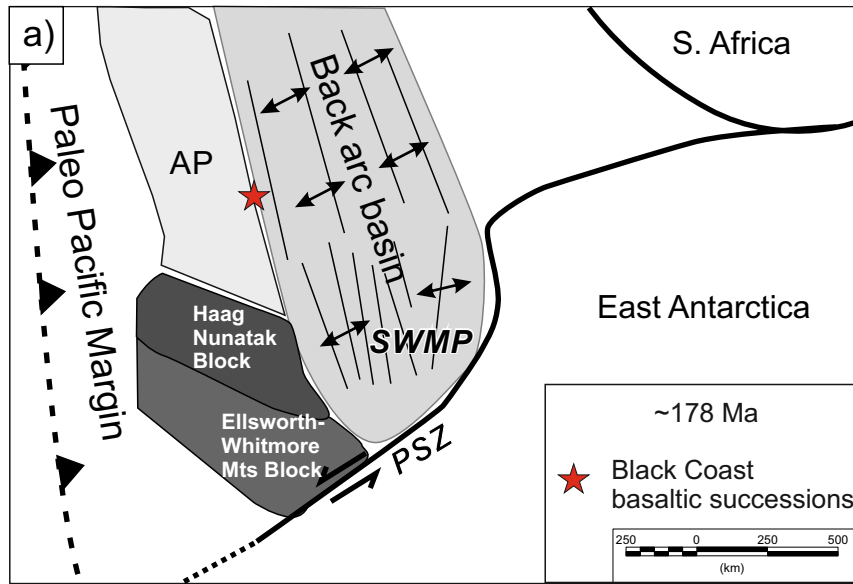


Figure 4



Figure 5

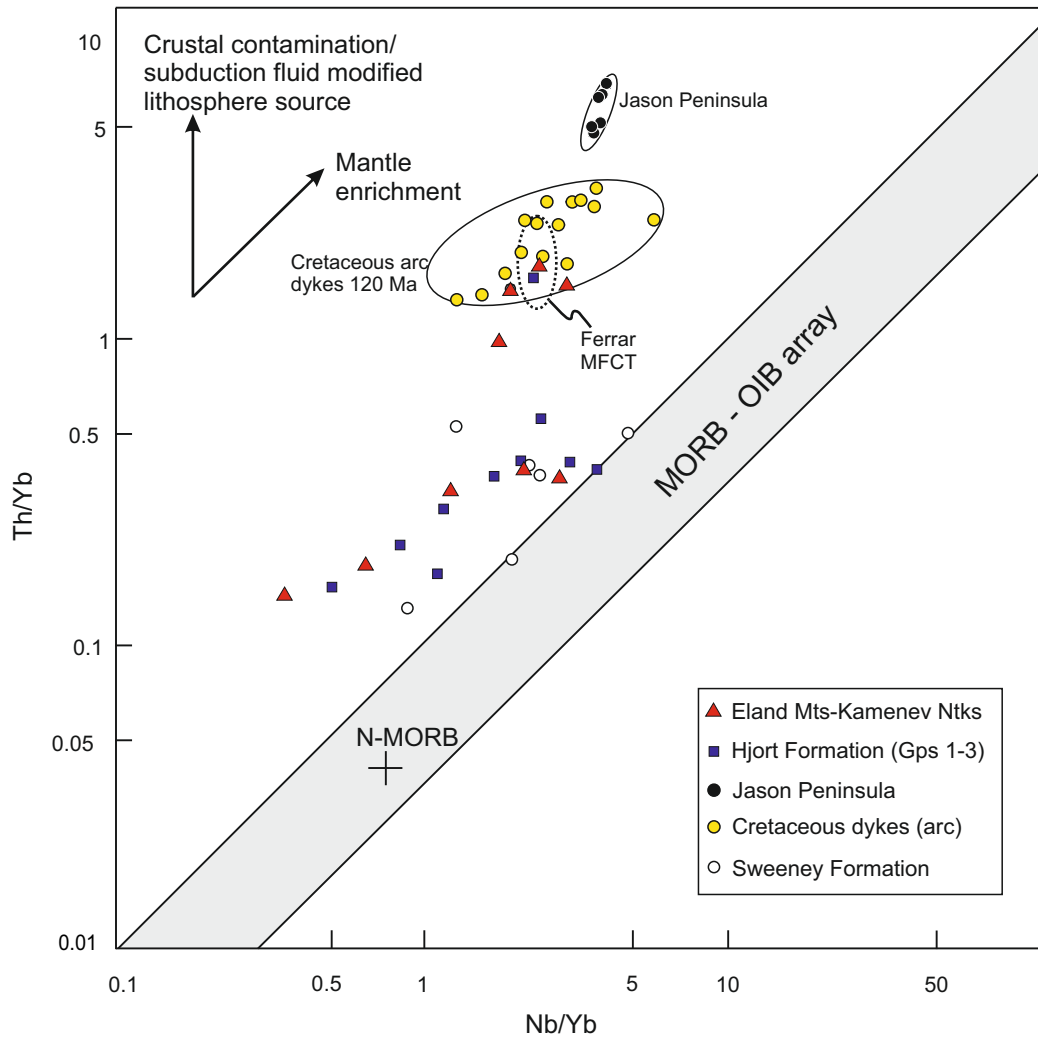


Figure 6

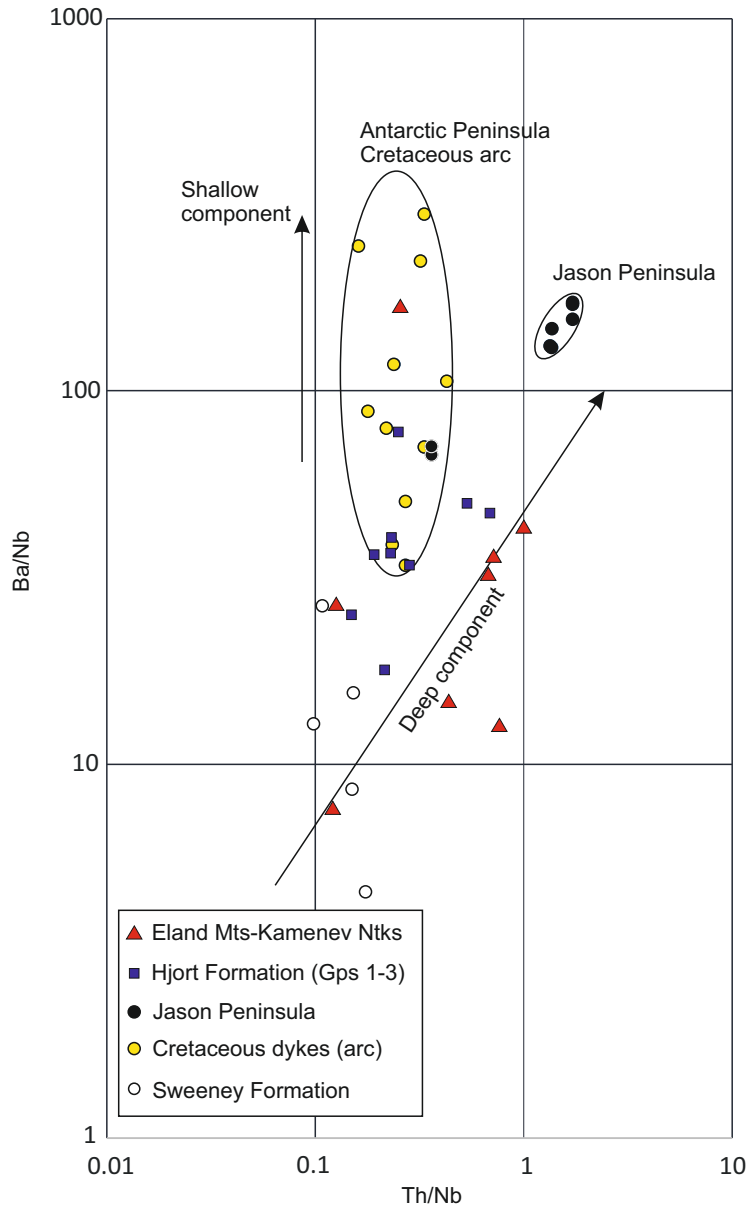


Figure 7

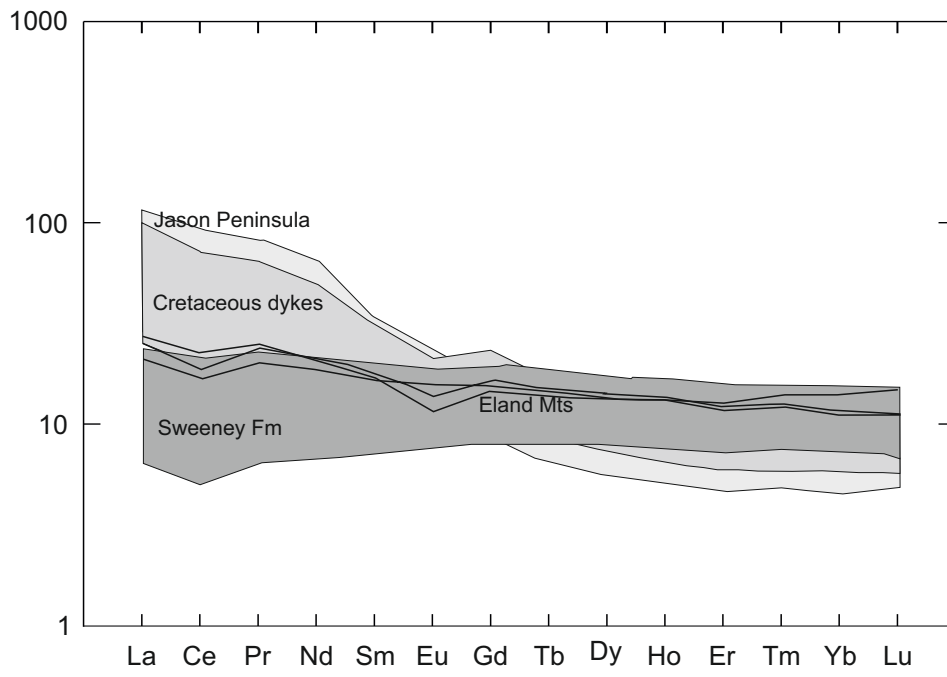


Figure 8

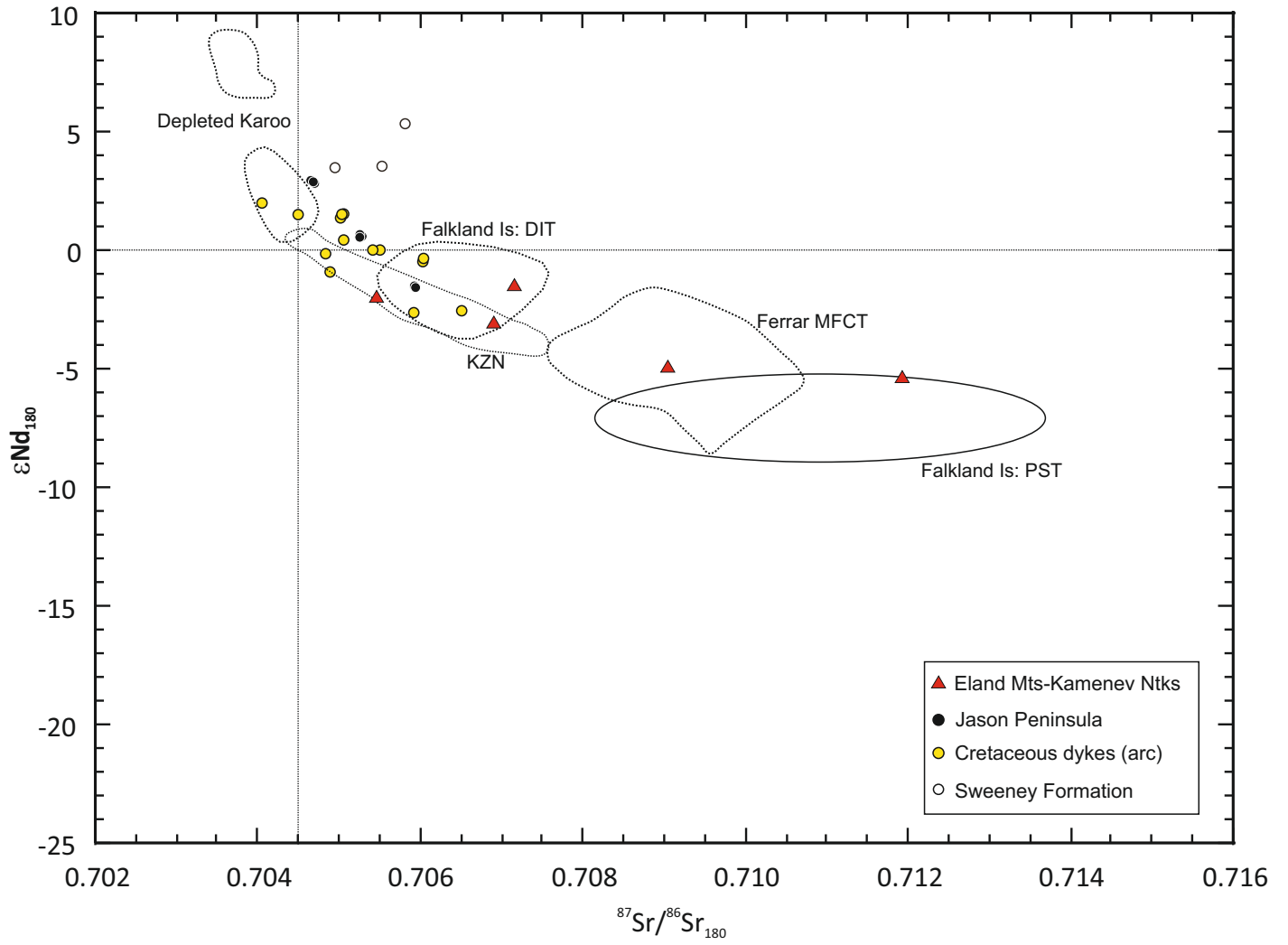


Figure 9